X-742-73-288
PREPRINT

NASA TM X- 70474

PRELIMINARY GUIDED ROCKET FEASIBILITY STUDY

(NASA-TM-X-70474) PRELIMINARY GUIDED ROCKET FEASIBILITY STUDY (NASA) 13 p HC $3.00 CSCL 16B
N73-32780
Unclas
G3/31 18558

MARK B. NOLAN
JOHN J. CELMER

SEPTEMBER 1973

GSFC
GODDARD SPACE FLIGHT CENTER
GREENBELT, MARYLAND

X-742-73-288

PRELIMINARY GUIDED ROCKET FEASIBILITY STUDY

Mark B. Nolan
John J. Celmer

September 1973

GODDARD SPACE FLIGHT CENTER
Greenbelt, Maryland

i

PRECEDING PAGE BLANK NOT FILMED

CONTENTS

ILLUSTRATIONS

ILLUSTRATIONS (Continued)

TABLES

PRELIMINARY GUIDED ROCKET FEASIBILITY STUDY

Mark B. Nolan, Aerospace Technologist
John J. Celmer, Aerospace Technologist
NASA Goddard Space Flight Center
Greenbelt, Maryland 20771

Abstract

The feasibility of actively guiding sounding rockets to reduce impact dispersion has been investigated. The theoretical probability of Range Safety thrust termination for several high performance rockets was combined with the cost of acquiring the extended range at White Sands Missile Range (WSMR) to establish a guidance system price ceiling of $20K per flight. Guiding the Black Brant VC (BBVC) for the first five (5) seconds of flight results in sufficient dispersion reduction to impact within the standard range boundaries at WSMR. The guidance system thrust level required to statically control the vehicle to a nominal-wind weighted trajectory for five (5) seconds is between 150 - 200 pounds. The required thrust level increases significantly with increasing control periods. The adverse effect of guidance system weight on apogee performance can be minimized to approximately 0.03 statute mile per pound of guidance system by mounting system externally in canisters and jettisoning the system at guidance termination (approximately five seconds).

A six-degree-of-freedom trajectory program with guidance simulation capability has been developed and the equations are delineated in this paper. A simple guidance law which involves flying a constant inertial attitude for a specified length of time was utilized in three simulations with the BBVC vehicle. These simulations demonstrated that an excessive amount of guidance fuel and high thrust levels are required to control the vehicle in a 30 FPS wind. Other guidance laws which appear more promising will be investigated.

Introduction

The potential for flight termination at White Sands Missile Range (WSMR) has increased significantly with the advent of higher performance sounding rockets. The probability of flight termination has been somewhat alleviated by extending the range boundaries, as shown in Figure 1, for these high performance vehicles. There are two problems associated with the use of the extended range boundaries at WSMR. The first is an $18K to $45K per day range charge while the second is a significant reduction in the launch scheduling flexibility. A study is now underway to determine the feasibility of developing a control system for the Black Brant VC (BBVC) and Astrobee F vehicles to restrict the magnitude of the vehicle impact dispersion to within the standard range boundaries. The financial and technical feasibility study will be presented in the first half of this paper. The six-degree-of-freedom guided flight simulations and the trajectory program developed for these simulations will be presented in the second half of the paper.

Feasibility Study

Financial Feasibility

The proposed guidance system will be considered financially feasible if the savings per flight resulting from the system equal or exceed the cost of the proposed system. This analysis will be limited to determining the cost savings resulting from use of the guidance system. The vehicle impact dispersion radius and the off-range impact probability (cutdown probability) are presented in Table 1.

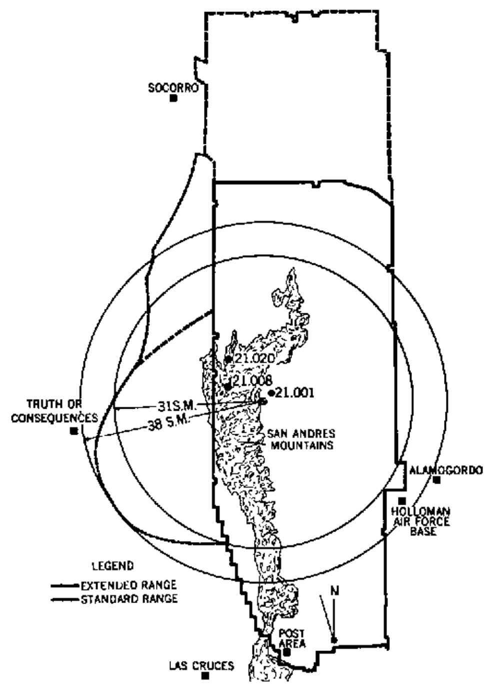

Figure 1. WSMR Range.

Table 1. Vehicle Dispersion and Off-Range Impact Probability

ROCKET VEHICLE*	PAYLOAD WEIGHT (LBS)	APOGEE ALTITUDE (ST. MI.)	3σ DISPERSION RADIUS (ST. MI.)	OFF-RANGE IMPACT PROBABILITIES: NORMAL DISTRIBUTION, EXTENDED BOUNDARIES	NORMAL DISTRIBUTION, STANDARD BOUNDARIES	BINORMAL DISTRIBUTION, EXTENDED BOUNDARIES	BINORMAL DISTRIBUTION, STANDARD BOUNDARIES
BLACK BRANT VC	500	180	38.0	2.2%	11.0%	6.8%	24.0%
BLACK BRANT VC	420	200	42.2	3.8	15	10.4	28.7
BLACK BRANT VC	300	240	50.6	6	20	18	36
ASTROBEE F	366	186	31.8	1	6.2	2.8	15.8
ASTROBEE F	320	200	34.2	1.3	7.9	4.1	19
AEROBEE 350	875	163	34.1	1.2	7.8	4.0	18.9
AEROBEE 350		200	41.8	3.5	14	9.9	29
AEROBEE 170	FLIGHT DATA	120-140	14.4	0	1	1	3
AEROBEE 200**	500	120	15	0	1	1	3
AEROBEE 200**	240	200	25	1	2.5	1	7.4

* ALL VEHICLES ARE TOWER LAUNCHED FROM WSMR.
**NUMBERS ARE AN ESTIMATION ON A NEW VEHICLE; NO DISPERSION ANALYSIS COMPLETED.
A FOUR MILE BUFFER ASSUMED IN ALL CALCULATIONS.

The dispersions values presented are theoretical for all vehicles with the exception of the Aerobee 170. The dispersion for the BBVC, Astrobee F, and Aerobee 200 are unproven due to lack of a significant number of flights. As can be seen in Table 1, two statistical techniques have been employed to generate the vehicle cutdown probabilities. The normal distribution method has been used in-house to date while the binormal distribution has recently been proposed by one of the vehicle contractors as a more rigorous approach. The normal distribution data will be used in this study for two reasons: (1) dispersion flight data for the Aerobee 170 vehicle correlates better with the normal distribution, and (2) the normal distribution results in the least money available for the guidance system.

The nominal vehicle launch costs (combined vehicle and payload cost) for each rocket type are estimated in Table 2. The mean launch cost for the BBVC and Astrobee F ($375K per vehicle) may be low considering the expensive telescopes and pointing systems that are often flown. The cost of vehicle cutdown prorated per launch is also presented in Table 2. Prorating the cost of vehicle cutdown on a per launch basis assumes that a sufficient number of vehicles is launched to amortize the cost. The first two BBVC flights used all range extension at WSMR at a cost of $45K per day. All subsequent flights have used only the western range extensions which cost approximately $18K per day. Since the proposed guidance system will reduce the cutdown probability to zero on the standard range, the cost savings for each vehicle will be the extended range cost plus the cutdown cost. The cost savings are presented in Figure 2 for the vehicles under consideration as a function of apogee altitude.

Table 2. Vehicle Cut-Down Cost

ROCKET VEHICLE	APOGEE ALTITUDE (st. mi.)	VEHICLE COST (thousands of dollars)	LAUNCH COST (thousands of dollars)	PRORATED VEHICLE CUT DOWN COST* NORMAL DISTRIBUTION EXTENDED BOUNDARIES (dollars)	NORMAL DISTRIBUTION STANDARD BOUNDARIES (dollars)	BINORMAL DISTRIBUTION EXTENDED BOUNDARIES (dollars)	BINORMAL DISTRIBUTION STANDARD BOUNDARIES (dollars)
BLACK BRANT VC	180	50	250–500	8,250	41,250	25,500	90,000
BLACK BRANT VC	200	50	250–500	14,250	56,250	39,000	111,375
BLACK BRANT VC	240	50	250–500	22,500	75,000	60,000	135,000
ASTROBEE F	186	50	250–500	3,750	23,250	10,500	59,250
ASTROBEE F	200	50	250–500	4,875	29,625	15,375	71,250
AEROBEE 350	163	200	500–1000	7,000	58,000	30,000	141,000
AEROBEE 350	200	200	500–1000	26,250	105,000	74,250	217,500
AEROBEE 170	120–140	50	250–500	0	3,750	3,750	11,250
AEROBEE 200	120	50	250–500	0	3,750	3,750	11,250
AEROBEE 200	200	50	250–500	3,750	9,375	3,750	27,750

*PRORATED VEHICLE CUT-DOWN COST = OFF-RANGE IMPACT PROBABILITY X MEAN LAUNCH COST.

The guidance system will be financially feasible if it can be produced for approximately $20K per flight. At this price, the system would generate substantial cost savings for flights above 200 statute miles. The target cost of $20K per flight is in excess of the cost estimate received from one contractor. However, it is too early in the program to have a great deal of confidence in this cost estimate.

The above analysis does not associate a cost savings with the increased operational flexibility derived from not requiring the extended range boundaries for each launch.

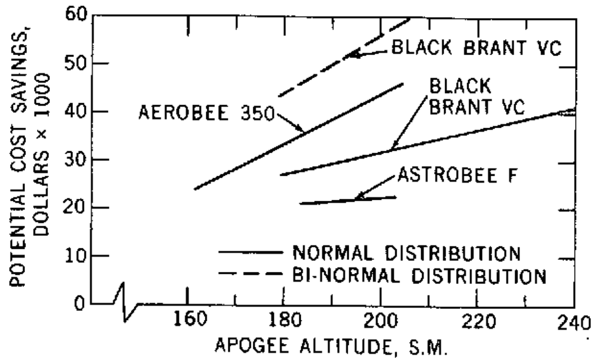

Figure 2. Potential Cost Savings Before Guidance Cost

Acquisition of the extended range boundaries is restricted by the request lead time, turn around time for cancelled launches, and relative program priorities. No attempt has been made to associate a dollar value with the logistics of requiring the extended range boundaries.

Technical Feasibility

This analysis will be restricted to three areas: (1) establishing the relationship between guidance duration and dispersion reduction, (2) calculating the guidance force required to statically control the rocket, and (3) defining the effect of several guidance packaging techniques on the vehicle performance. It is assumed that the guidance system is initiated at launch tower exit (approximately 1.5 seconds); thus the duration of guided flight begins at lift-off and continues to guidance termination.

The BBVC vehicle will be used as a model for this study. The vehicle apogee performance from WSMR (QE = 88 degrees) is presented in Figure 3 for both the 3 to 1 and the 4.25 to 1 ogive nose cones. In the remaining analysis, a 500 pound gross payload with the 3 to 1 ogive nose will be used. The first 60 seconds of the nominal trajectory are presented in Figure 4.

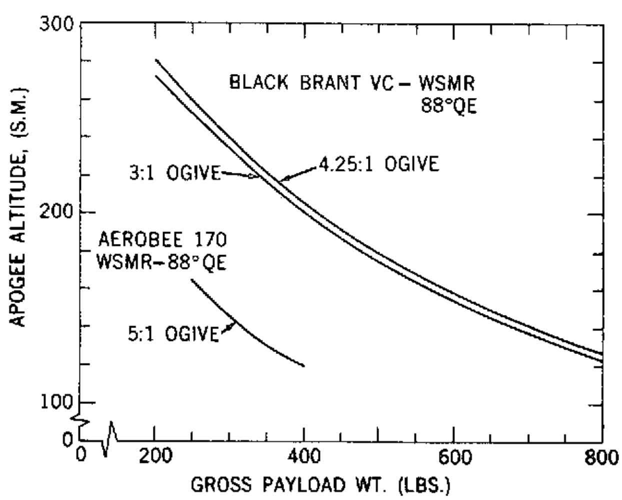

Figure 3. Apogee Altitude Performance

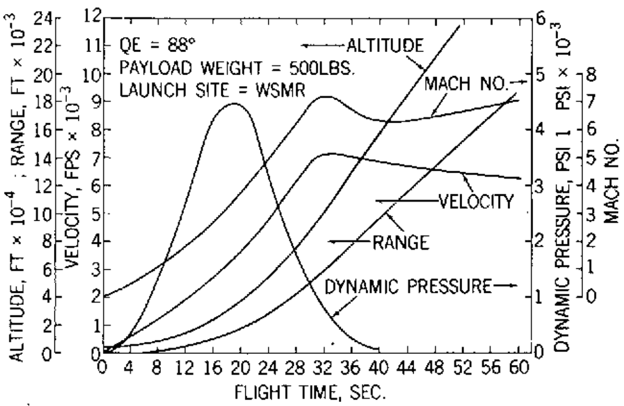

Figure 4. Black Brant VC Trajectory Parameters

Relationship Between Guidance Deviation and Dispersion Reduction

A current estimate of the BBVC vehicle impact dispersion at WSMR is presented in Table 3. The three sigma in-range dispersion radius for the BBVC vehicle is 38 statute miles. Over 99.5 percent of the total dispersion, 37.6 statute miles, is the result of unknown winds and thrust misalignments as shown in Table 3. The dispersion resulting from both of these sources is generated very early in flight and, therefore, the dispersion from these sources could be virtually eliminated or at least significantly reduced by controlling the vehicle motion during the initial seconds of flight.

Table 3. Theoretical Impact Dispersion

VEHICLE : BLACK BRANT VC
LAUNCH SITE : WHITE SANDS MISSILE RANGE
GROSS PAYLOAD WEIGHT : 500 POUNDS
QE : 88 DEGREES

DISPERSION SOURCE	3 σ MAGNITUDE OF SOURCE	IN-RANGE DISPERSION (ST. MI.)	ACCUMULATIVE DISPERSION RADIUS
UNKNOWN WIND (FPS)	7.5	30.8	30.8
THRUST MISALIGNMENT (DEG)	0.2	21.6	37.62
FIN MISALIGNMENT (DEG)	0.2	3.28	37.76
DRAG ERROR	10%	0.73	37.77
IMPULSE ERROR	2%	3.17	37.90
WEIGHT ERROR (LBS)	5	0.22	37.90
TOWER SETTING ERROR (ELEVATION–DEG)	0.1	2.0	37.96
TOTAL IN-RANGE DISPERSION*)			37.96 ST. MI.

*TOWER TIP-OFF IS NO LONGER INCLUDED IN THE DISPERSION SINCE NONE HAS BEEN EXPERIENCED ON THE FIRST FIVE FLIGHTS (two flights from Wallops Island and three from White Sands Missile Range).

The ballistic wind function which defines the relative response of the vehicle to winds as a function of altitude is presented in Figure 5. This figure indicates that half of the vehicle response (impact displacement) to a ballistic wind will occur in the first 500 feet of flight and 62 percent of the vehicle response will occur in the first 850 feet or 4.0 seconds of flight. The dispersion due to the unknown wind is presented in Figure 6 as a function of guided flight time. In this figure, it is assumed that guidance is perfect; therefore, the vehicle flies an undisturbed trajectory during the guided portion of flight. The dispersion factor, wind in this case, is introduced at guidance termination. The same effect can be seen in Figure 7 for the dispersion due to thrust misalignment. The dispersion due to thrust misalignment decreases more rapidly with guidance time than the dispersion due to unknown wind because of the effect of vehicle roll rate and increasing dynamic pressure. The reduction in total vehicle dispersion as a function of guidance time is presented in Figure 8. Note that the dispersion radius reaches a lower limit of five miles which is due to the five remaining dispersion parameters. Of these five factors, only the dispersion due to fin misalignment could be reduced by the proposed system. The theoretical minimum dispersion radius is approximately four statute miles. However, it is not necessary to reduce the dispersion to this minimum value. An acceptable dispersion radius would be fifteen statute miles. Approximately four seconds (Figure 8) of guidance would be needed to reduce the dispersion radius to fifteen statute miles.

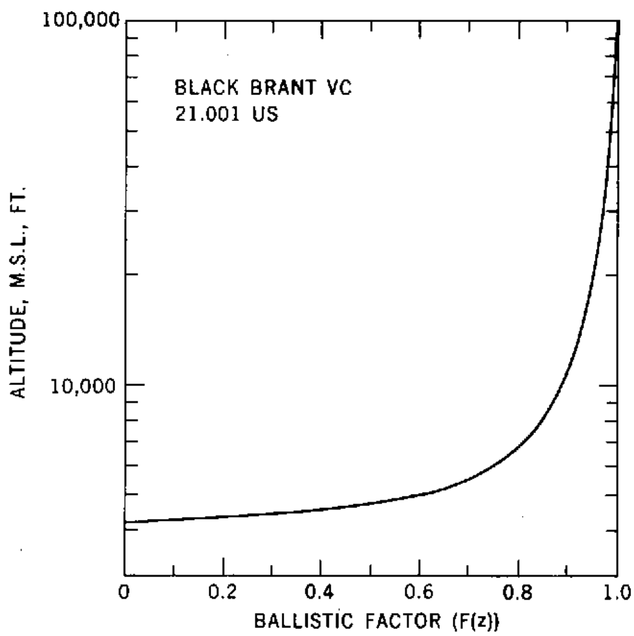

Figure 5. Ballistic Factor

Again it should be noted that this is a preliminary estimate of the guidance effects and does not include the dispersion due to guidance system errors such as angle measurement accuracy, magnitude of the angular dead band, and the dynamics of the response to in-flight perturbation. This information will be derived at a later date in a more detailed analysis where particular guidance laws and hardware concepts will be analyzed. The dispersion due to the guidance system itself should pose no problem. The guided flight time can be varied to control the dispersion of the Table 1 parameters so that the overall dispersion (including that due to the guidance system) can be held within the fifteen mile limit.

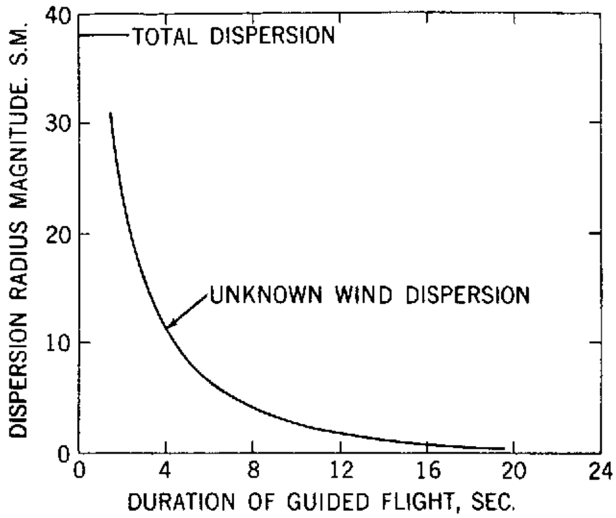

Figure 6. Wind Dispersion

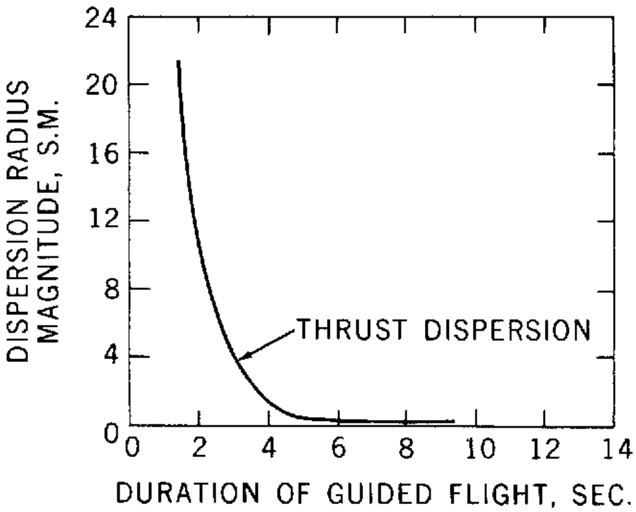

Figure 7. Thrust Dispersion

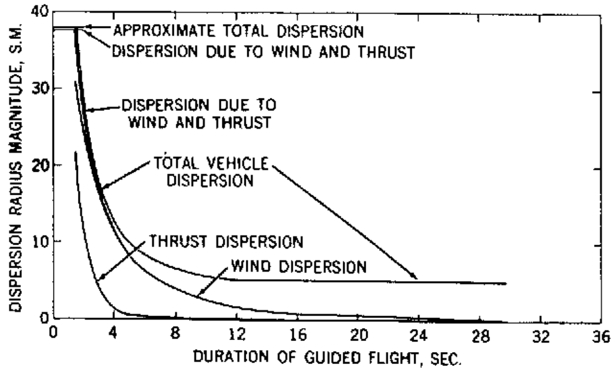

Figure 8. Black Brant VC — Guidance Study

Guidance Forces Necessary to Control Rocket

The torque generated by each of the three controllable dispersion parameters (unknown wind, thrust misalignment and fin misalignment) is presented in Figure 9. The total torque was calculated by taking a square root of the sum of the squares of the individual torques similar to combining the dispersion parameters. The guidance force necessary to statically control the vehicle is presented in Figure 10 as a function of point of application along the rocket for constant times. The above control force is also presented in Figure 11 for specific locations as a function of time. A force of 250 pounds located at the nozzle exit plane or 200 pounds at the base of the nose cone is sufficient to statically control the rocket for the first eight seconds of flight. The force level necessary to dynamically control the rocket is a function of the guidance law employed and will be calculated in future analysis.

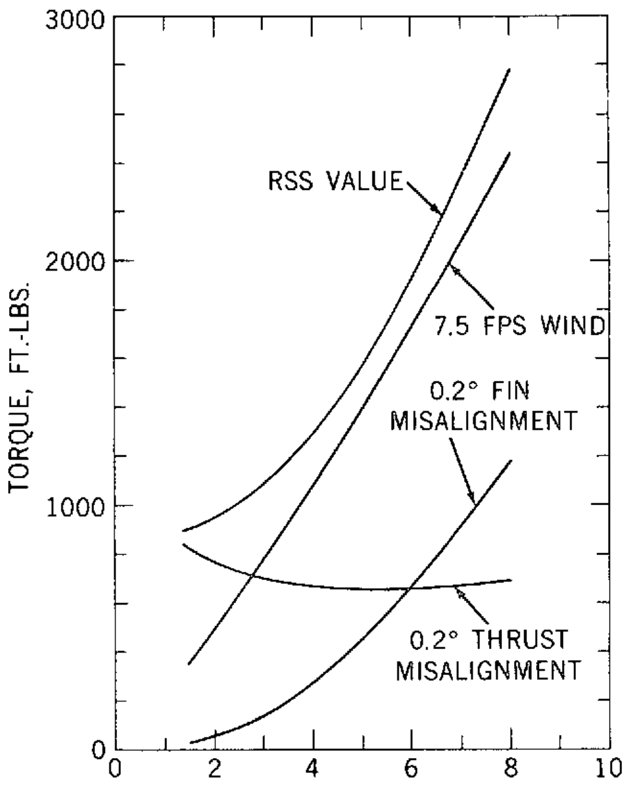

Figure 9. Torques Generated By Dispersion Parameters (3σ Level)

Guidance System Effect on Performance

The next major question is the effect of the guidance system on the vehicle performance. The most often mentioned guidance configuration is to mount the system in the payload which means it will have to be carried to apogee. If the system is mounted in canisters on the aft

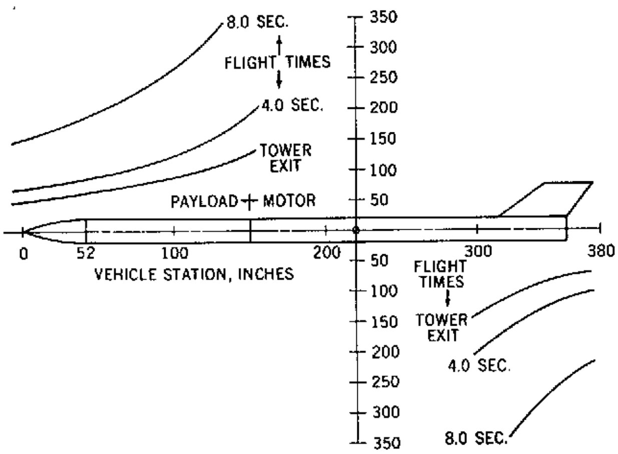

Figure 10. Force Required to Statically Control 3σ Dispersion Moments & Vehicle Station for Constant Flight Times

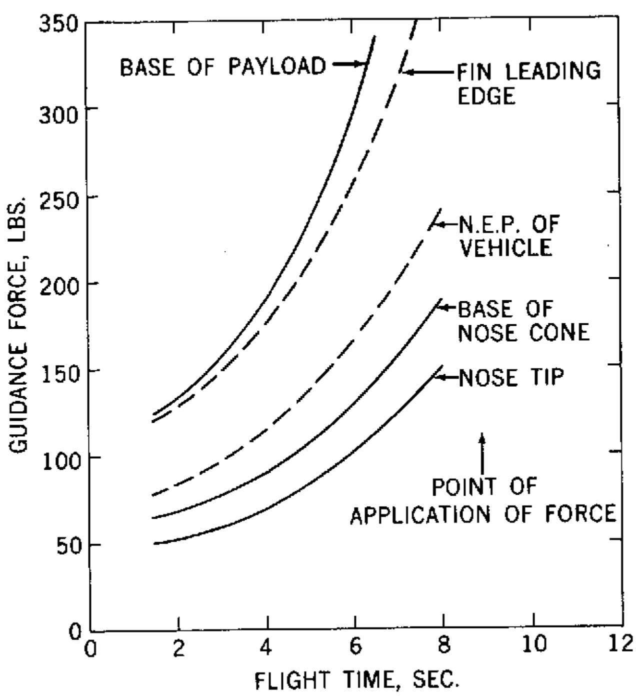

Figure 11. Force Required to Statically Control 3σ Dispersion Moments & Time for Constant Vehicle Stations

of the vehicle, the guidance package can be jettisoned after guidance termination (within the first ten seconds of flight). Figure 12 presents the loss in apogee altitude per pound of guidance system as a function of the jettison time. Jettison time corresponds to guidance termination. The data is presented for no drag increase during the guided phase and for double the nominal vehicle drag during the guided phase. For the nominal drag configuration, the apogee loss is 0.04 mile for each pound of guidance system if jettisoned at ten seconds. The apogee

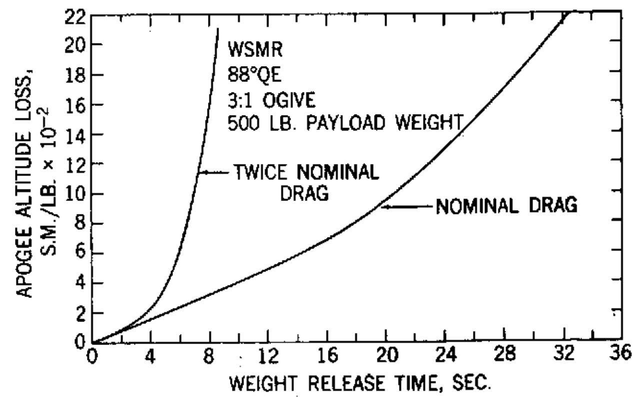

Figure 12. Black Brant VC — Guidance Study

loss for carrying the guidance module to apogee is approximately 0.22 mile per pound. The apogee loss for carrying the weight to apogee is over five times greater than jettisoning at ten seconds. The jettisonable weight as a function of the jettison time that has an equivalent apogee altitude loss of one pound carried to apogee is presented in Figure 13. This data is presented for both nominal and twice nominal drag during the guided phase of flight. As can be seen, jettisoning the guidance system drastically reduces the system impact on vehicle performance. This is particularly significant since the guidance system weights have been estimated between 50 and 70 pounds.

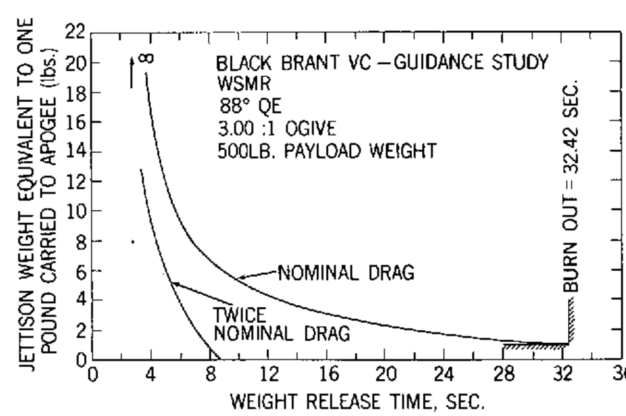

Figure 13. Black Brant VC — Guidance Study

Summary.

A significant reduction in the impact dispersion can be achieved by guiding the BBVC vehicle during the initial seconds of flight. Sufficient dispersion reduction can be achieved to fly on the standard range at WSMR. Further if the guidance is contained in canisters attached between the fins and jettisoned at guidance termination, the loss in apogee performance is minimal. For a 50 pound guidance system, the apogee loss would be 1.4 miles if the canisters are jettisoned at 7.0 seconds. If carried to apogee, the loss would be 10 miles.

Computer Simulations

A six-degree-of freedom digital computer program was written in Fortran by the use of the "Model" translator and run on an XDS 9300 computer. The vehicle is assumed to be a symmetric rigid body with negligible products of inertia. The vehicle is inherently stable aerodynamically. The fins are canted to introduce an increasing roll rate which will reduce the error due to thrust misalignment. The equations used in the simulation are listed in the section on System Equations. A spherical earth is assumed. The variable coefficients which are functions of either mach number, time or altitude are entered in tabular form and linear interpolation is used.

The translation forces are computed in body coordinates and the accelerations are integrated to yield the translational velocities in the body frame. The velocities are transformed to inertial coordinates and integrated to yield the rectangular coordinates of the position. From the position coordinates the altitude, longitude and latitude relative to a rotating spherical earth are calculated and used to define a geocentric coordinate system. The torques are computed in body coordinates and the angular accelerations are integrated to yield the angular velocities in the body frame. The angular velocities are used in a set of nine kinematical differential equations which yield the direction cosines relating the body frame to the inertial reference frame. The gravity and wind forces are defined in the geocentric coordinate system then transformed into inertial components and then finally resolved into the body frame.

The first control scheme to be evaluated uses reaction jets to hold the nominal thrust axis at an inertial reference to coincide with the initial launch attitude. A frictionless free gyro is used to measure the inertial reference axis and is defined explicitly by two gimbal angles. The outer gimbal represents pitch motion and the inner gimbal represents the yaw angle. Reaction jets are fired in each axis for the purpose of holding the gimbal angles below or near a small threshold.

Computer Results

From the data of Figure 9 it was estimated that a torque of 5600 ft. lb. is required to control the vehicle in the presence of a 30 ft/sec wind. A series of runs were made using that torque level and winds of 30, 20 and 10 ft/sec. A minimum on time of 10 milliseconds was assumed for the jet. The control is programmed to cut off after 5 sec. The transient response of the vehicle was recorded on a strip chart recorder. The following runs were completed:

Run #	Control Torque	Wind
1	5600 ft. lb.	30 ft/sec from the east
2	5600	20 " " " "
3	5600	10 " " " "
4	0	20
5	0	0
6	5600	20 ft/sec from the north
7	5600	30

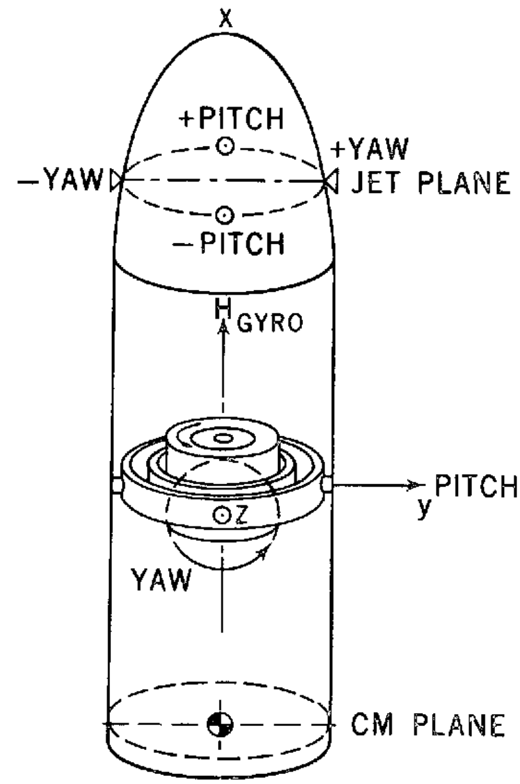

Figure 14. Gyro Configuration

The vehicle was launched due east with an elevation of 88 Deg. Run 5 was made with ideal conditions and showed that the pitch angle after 5 sec due to gravity with no control torque is 0.35 Deg. Run 4 was run with a 20 ft/sec wind but no control and showed that the pitch angle after 1 sec is 5 Deg. The transients from runs 1, 2 and 3 are included in this report.

The following variables are presented.

Channel Number	Variable	Full Scale Value ±	Symbol
1	Pitch Angle	.5 Deg.	θ
2	Pitch Control Torque	6000 ft. lb.	M_{yc}
3	Pitch Aerodynamic Moment	5000 ft. lb.	M_{yB}
4	Total Angle of Attack	10 Deg.	δ
5	Yaw Angle	.5 Deg.	ψ
6	Yaw Control Torque	6000 ft. lb.	M_{zc}
7	Yaw Aerodynamic Moment	5000 ft. lb.	M_{zB}

An observation of the recordings reveal that the jets will fire as expected with a duty cycle proportional to the aerodynamic torque in each axis. However the frequency of firings depends on the initial conditions as well as the aerodynamic torque. The frequencies observed in the computer runs vary from 3 to 20 Hertz. The amplitude of error for each run did not exceed .06 Deg. above the threshold of .1 Deg. The total error is ±.16 Deg. The errors could be reduced by lowering the threshold however large tip off rates would produce excessive jet firings. The greatest disadvantage of holding an inertial attitude during the launch is the requirement for a large control torque and a large fuel consumption and the frequency and level of the resulting structural loads. The greatest advantage is the ease of implementation and fine accuracy.

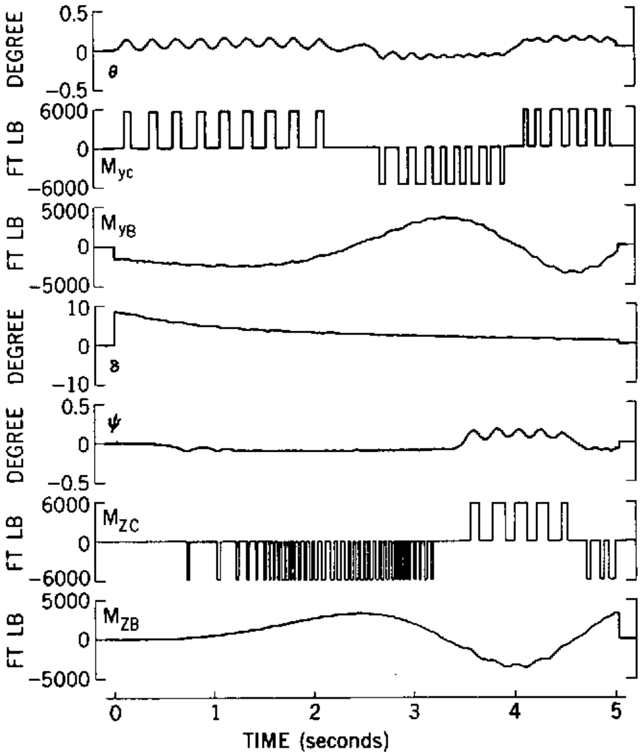

Figure 15. Flight Simulation, 30 FPS Wing, Run 1, January 4, 1973

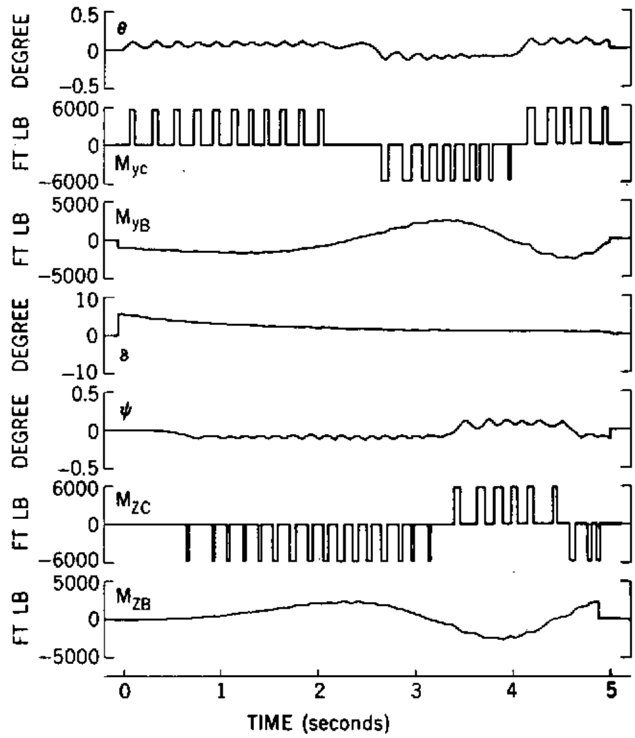

Figure 16. Flight Simulation, 20 FPS Wind, Run 2

Fuel Consumption

The fuel requirements for 5 sec of control in the pitch axis are given in the following table:

Run #	Fuel (ft. lb. sec.)	Total Jet On Time	Wind Velocity
1	10192	1.82 sec.	30 ft/sec
2	7448	1.33 sec.	20
3	3976	.71 sec.	10

Since the vehicle is rolling (3.5 rad/sec after 5 sec) there is a simular requirement for fuel in the yaw axis.

Conclusion

An inertial control system has the advantage of ease of implementation, high accuracy, reduced wind sensitivity and the disadvantage of high fuel consumption and high structural load levels. The ultimate choice will depend on a future study of the feasibility of a nominal trajectory control system. The trajectory control system has the advantage of low fuel and low torque requirements and the disadvantage of complexity and high sensitivity to large sudden wind variations.

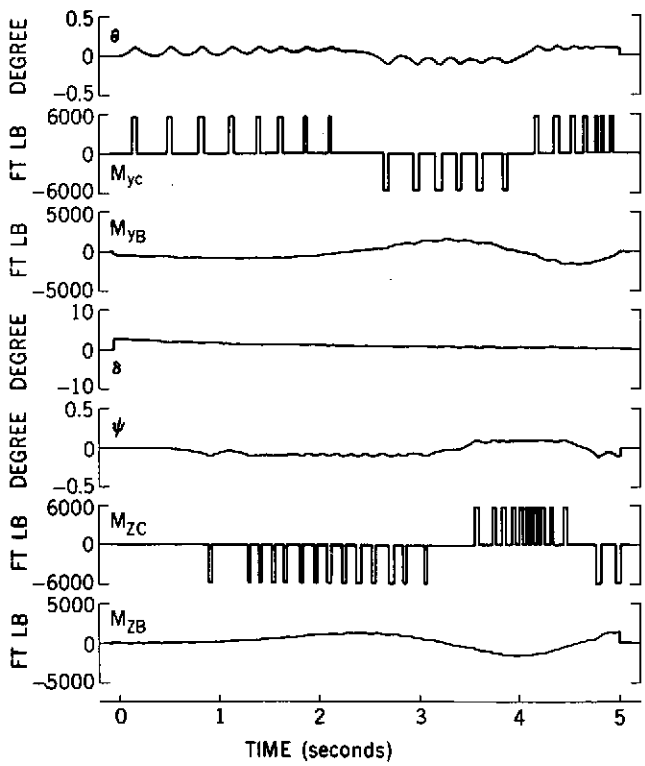

Figure 17. Flight Simulation, 10 FPS Wind, Run 3

System Equations

Translational Dynamics

$$\dot{u} = \frac{1}{m}\left[F_{XB} + F_{XT} + F_{XC}\right] + g_X - Qw + Rv$$

$$\dot{v} = \frac{1}{m}\left[F_{YB} + F_{YT} + F_{YC}\right] + g_z - Ru + Pw$$

$$\dot{w} = \frac{1}{m}\left[F_{ZB} + F_{ZT} + F_{ZC}\right] + g_z - Pv + Qu$$

Rotational Dynamics

$$\dot{P} = \frac{1}{I_X}\left[M_{XB} + M_{XT} + M_{XC}\right] - QR\left(I_Z - I_Y\right)/I_X$$

$$\dot{Q} = \frac{1}{I_Y}\left[M_{YB} + M_{YT} + M_{YC}\right] - PR\left(I_X - I_Z\right)/I_Y$$

$$\dot{R} = \frac{1}{I_Z}\left[M_{ZB} + M_{ZT} + M_{ZC}\right] - PQ\left(I_Y - I_X\right)/I_Z$$

Kinematics

$$\begin{pmatrix} \dot{a}_{11} & \dot{a}_{12} & \dot{a}_{13} \\ \dot{a}_{21} & \dot{a}_{22} & \dot{a}_{23} \\ \dot{a}_{31} & \dot{a}_{32} & \dot{a}_{33} \end{pmatrix} = \begin{pmatrix} a_{11} & a_{12} & a_{13} \\ a_{21} & a_{22} & a_{23} \\ a_{31} & a_{32} & a_{33} \end{pmatrix} \begin{pmatrix} O & -R & Q \\ R & O & -P \\ -Q & P & O \end{pmatrix}$$

Coordinate Transformation (body to inertial, velocity vector)

$$\begin{pmatrix} U \\ V \\ W \end{pmatrix} = \begin{pmatrix} a_{11} & a_{12} & a_{13} \\ a_{21} & a_{22} & a_{23} \\ a_{31} & a_{32} & a_{33} \end{pmatrix} \begin{pmatrix} u \\ v \\ w \end{pmatrix}$$

Inertial Displacement

$$\dot{x} = U$$
$$\dot{y} = V$$
$$\dot{z} = W$$

Coordinates Relative to the Earth (longitude λ, latitude φ)

$$\tan\left(\lambda + \Lambda_E\right) = \frac{Y}{X}$$

$$\tan\varphi = \frac{Z}{\sqrt{X^2 + Y^2}}$$

$$R = \sqrt{X^2 + Y^2 + Z^2}$$

$$ALT = R - R_E$$

Initial Conditions

Translational velocities

$$\begin{pmatrix} u(0) \\ v(0) \\ w(0) \end{pmatrix}_{BODY} = \begin{pmatrix} a_{11}(0) & a_{21}(0) & a_{31}(0) \\ a_{12}(0) & a_{22}(0) & a_{32}(0) \\ a_{13}(0) & a_{23}(0) & a_{33}(0) \end{pmatrix} X \begin{bmatrix} -R_E\ \omega_E \operatorname{Cos}(\varphi(0)) \operatorname{Sin}(\lambda(0)) + \Lambda_E(0) \\ R_E\ \omega_E \operatorname{Cos}(\varphi(0)) \operatorname{Cos}(\lambda(0)) + \Lambda_E(0) \\ 0 \end{bmatrix}_{INERTIAL}$$

Displacement

$$X(0) = R_E \operatorname{Cos}(\varphi(0)) \operatorname{Cos}(\lambda(0) + \Lambda_E(0))$$
$$Y(0) = R_E \operatorname{Cos}(\varphi(0)) \operatorname{Sin}(\lambda(0) + \Lambda_E(0))$$
$$Z(0) = R_E \operatorname{Sin}\varphi(0)$$

Angular Velocity

$$\begin{pmatrix} P(0) \\ Q(0) \\ R(0) \end{pmatrix} = \begin{pmatrix} a_{11}(0) & a_{21}(0) & a_{31}(0) \\ a_{12}(0) & a_{22}(0) & a_{32}(0) \\ a_{13}(0) & a_{23}(0) & a_{33}(0) \end{pmatrix} \begin{pmatrix} O \\ O \\ \omega_E \end{pmatrix}_{INERTIAL}$$

Direction Cosines (Azimuth Λ, Elevation T)

$$\begin{aligned} a_{11}(0) = {} & \operatorname{Cos}(\lambda(0)) \operatorname{Cos}(\varphi(0)) \operatorname{Sin}(T(0)) \\ & - \operatorname{Cos}(\lambda(0)) \operatorname{Sin}(\varphi(0)) \operatorname{Cos}(\Lambda(0)) \operatorname{Cos}(T(0)) \\ & - \operatorname{Sin}(\lambda(0) \operatorname{Sin}(\Lambda(0)) \operatorname{Cos}(T(0)) \end{aligned}$$

$$a_{12}(0) = \operatorname{Cos}(\lambda(0)) \operatorname{Sin}(\varphi(0)) \operatorname{Sin}(\Lambda(0)) - \operatorname{Sin}(\lambda(0)) \operatorname{Cos}(\Lambda(0))$$

$$\begin{aligned} a_{13}(0) = {} & - \operatorname{Cos}(\lambda(0)) \operatorname{Cos}(\varphi(0)) \operatorname{Cos}(T(0)) \\ & - \operatorname{Cos}(\lambda(0)) \operatorname{Sin}(\varphi(0)) \operatorname{Cos}(\Lambda(0)) \operatorname{Sin}(T(0)) \\ & - \operatorname{Sin}(\lambda(0)) \operatorname{Sin}(\Lambda(0)) \operatorname{Sin}(T(0)) \end{aligned}$$

$$\begin{aligned} a_{21}(0) = {} & \operatorname{Sin}(\lambda(0)) \operatorname{Cos}(\varphi(0)) \operatorname{Sin}(T(0)) \\ & - \operatorname{Sin}(\lambda(0)) \operatorname{Sin}(\varphi(0)) \operatorname{Cos}(\Lambda(0)) \operatorname{Cos}(T(0)) \\ & + \operatorname{Cos}(\lambda(0)) \operatorname{Sin}(\Lambda(0)) \operatorname{Cos}(T(0)) \end{aligned}$$

$$a_{22}(0) = \operatorname{Sin}(\lambda(0)) \operatorname{Sin}(\varphi(0)) \operatorname{Sin}(\Lambda(0)) + \operatorname{Cos}(\lambda(0)) \operatorname{Cos}(\Lambda(0))$$

$$\begin{aligned} a_{23}(0) = {} & - \operatorname{Sin}(\lambda(0)) \operatorname{Cos}(\varphi(0)) \operatorname{Cos}(T(0)) \\ & - \operatorname{Sin}(\lambda(0)) \operatorname{Sin}(\varphi(0)) \operatorname{Cos}(\Lambda(0)) \operatorname{Sin}(T(0)) \\ & + \operatorname{Cos}(\lambda(0)) \operatorname{Sin}(\Lambda(0)) \operatorname{Sin}(T(0)) \end{aligned}$$

$$a_{31}(0) = \operatorname{Sin}(\varphi(0)) \operatorname{Sin}(T(0)) + \operatorname{Cos}(\varphi(0)) \operatorname{Cos}(\Lambda(0)) \operatorname{Cos}(T(0))$$

$$a_{32}(0) = - \operatorname{Cos}(\varphi(0)) \operatorname{Sin}(\Lambda(0))$$

$$a_{33}(0) = - \operatorname{Sin}(\varphi(0)) \operatorname{Cos}(T(0)) + \operatorname{Cos}(\varphi(0)) \operatorname{Cos}(\Lambda(0)) \operatorname{Sin}(T(0))$$

Gyro Reference Axis (initial X axis of vehicle)

$$\vec{S} = \begin{pmatrix} a_{11}(0) \\ a_{21}(0) \\ a_{31}(0) \end{pmatrix}_{\text{INERTIAL}}$$

Gyro Reference Axis (in terms of gimbal angles; pitch outer; yaw inner)

$$\vec{S} = \begin{pmatrix} \operatorname{Cos}\Psi_g \operatorname{Cos}\Theta_g \\ \operatorname{Sin}\Psi_g \\ -\operatorname{Cos}\Psi_g \operatorname{Sin}\Theta_g \end{pmatrix}_{\text{BODY}}$$

Gyro Reference Axis (in terms of direction cosines)

$$\vec{S} = \begin{pmatrix} S_X \\ S_Y \\ S_Z \end{pmatrix}_{\text{BODY}} = \begin{pmatrix} a_{11}\ a_{11}(0) + a_{21}\ a_{21}(0) + a_{31}\ a_{31}(0) \\ a_{12}\ a_{12}(0) + a_{22}\ a_{22}(0) + a_{32}\ a_{32}(0) \\ a_{13}\ a_{13}(0) + a_{23}\ a_{23}(0) + a_{33}\ a_{33}(0) \end{pmatrix}_{\text{BODY}}$$

Gimbal Angles

$$\tan\Theta_g = \frac{-S_Z}{S_X}$$

$$\operatorname{Sin}\Psi_g = S_Y$$

Transformation from Geocentric to Body Coordinates (T)

$$T = \begin{bmatrix} a_{11} & a_{21} & a_{31} \\ a_{12} & a_{22} & a_{32} \\ a_{13} & a_{23} & a_{33} \end{bmatrix} X$$

$$\begin{bmatrix} -\operatorname{Sin}(\varphi)\operatorname{Cos}(\lambda+\Lambda_E) & -\operatorname{Sin}(\lambda+\Lambda_E) & -\operatorname{Cos}(\varphi)\operatorname{Cos}(\lambda+\Lambda_E) \\ -\operatorname{Sin}(\varphi)\operatorname{Sin}(\lambda+\Lambda_E) & \operatorname{Cos}(\lambda+\Lambda_E) & -\operatorname{Cos}(\varphi)\operatorname{Sin}(\lambda+\Lambda_E) \\ \operatorname{Cos}(\varphi) & O & -\operatorname{Sin}(\varphi) \end{bmatrix}$$

Relative Wind

$$\begin{bmatrix} u_r \\ v_r \\ w_r \end{bmatrix}_{\text{BODY}} = \begin{bmatrix} u \\ v \\ w \end{bmatrix}_{\text{BODY}} -T \begin{bmatrix} O \\ R\ W_E \operatorname{Cos}(\varphi) \\ O \end{bmatrix}_{\text{GEOCENTRIC}} -T \begin{bmatrix} \text{North wind} \\ \text{East wind} \\ O \end{bmatrix}_{\text{GEOCENTRIC}}$$

Angle of Attact α and Sideslip β

$$\tan\alpha = \frac{w_r}{\sqrt{u_r^2 + v_r^2}} \qquad \tan\beta = \frac{v_r}{\sqrt{u_r^2 + w_r^2}}$$

Forces

$$\begin{aligned} F_{XB} &= -C_D\, q\, S \\ F_{YB} &= -C_{N\alpha} \operatorname{Sin}\beta\, q\, S \\ F_{ZB} &= -C_{N\alpha} \operatorname{Sin}\alpha\, q\, S \\ F_{XT} &= (T + A\Delta P)\operatorname{Cos}\epsilon \\ F_{YT} &= (T + A\Delta P)\operatorname{Sin}\epsilon \operatorname{Sin}\varphi \\ F_{ZT} &= (T + A\Delta P)\operatorname{Sin}\epsilon \operatorname{Cos}\varphi \end{aligned}$$

Moments

(Misalignment)

$$\begin{aligned} M_{XT} &= F_{ZT}\, Y_A - F_{YT}\, Z_A \\ M_{YT} &= F_{XT}\, Z_A - F_{ZT}\left(X_{cg} - X_A\right) + m_q\, Q \\ M_{ZT} &= F_{YT}\left(X_{cg} - X_A\right) - F_{XT}\, Y_A + n_r\, R \end{aligned}$$

(Aerodynamic)

$$M_{XB} = \left[C_{\ell\delta}\, S_F + C_{\ell p}\left(\frac{Pd}{2V_r}\right)\right] q\, S\, d$$

$$M_{YB} = \left[C_{N\alpha}\ \frac{\left(X_{cg} - X_{cp}\right)}{d}\ \operatorname{Sin}\alpha + C_{nq}\left(\frac{Qd}{2V_r}\right)\right] q\, S\, d$$

$$M_{ZB} = \left[-C_{N\alpha}\ \frac{\left(X_{cg} - X_{cp}\right)}{d}\ \operatorname{Sin}\beta + C_{nq}\left(\frac{Rd}{2V_r}\right)\right] q\, S\, d$$

$$q = \frac{1}{2}\ \varrho\, V_r^2$$

$$\text{MACH NUMBER} = \frac{V_r}{V_{\text{SOUND}}}$$